Crucial role for the LSP1–myosin1e bimolecular complex in the regulation of Fcγ receptor–driven phagocytosis

Sebastian Maxeiner[a], Nian Shi[a], Carmen Schalla[a], Guelcan Aydin[a], Mareike Hoss[b], Simon Vogel[c], Martin Zenke[a], and Antonio S. Sechi[a]

[a]Institute of Biomedical Engineering, Department of Cell Biology, and [b]Electron Microscopy Facility, Uniklinik RWTH Aachen, and [c]Fraunhofer Institute for Molecular Biology and Applied Ecology, D-52074 Aachen, Germany

ABSTRACT Actin cytoskeleton remodeling is fundamental for Fcγ receptor–driven phagocytosis. In this study, we find that the leukocyte-specific protein 1 (LSP1) localizes to nascent phagocytic cups during Fcγ receptor–mediated phagocytosis, where it displays the same spatial and temporal distribution as the actin cytoskeleton. Down-regulation of LSP1 severely reduces the phagocytic activity of macrophages, clearly demonstrating a crucial role for this protein in Fcγ receptor–mediated phagocytosis. We also find that LSP1 binds to the class I molecular motor myosin1e. LSP1 interacts with the SH3 domain of myosin1e, and the localization and dynamics of both proteins in nascent phagocytic cups mirror those of actin. Furthermore, inhibition of LSP1–myosin1e and LSP1–actin interactions profoundly impairs pseudopodial formation around opsonized targets and their subsequent internalization. Thus the LSP1–myosin1e bimolecular complex plays a pivotal role in the regulation of actin cytoskeleton remodeling during Fcγ receptor–driven phagocytosis.

INTRODUCTION

Cell motility and the associated cytoskeleton dynamics play a fundamental role in the regulation of several biological events, including embryonic development, wound healing, and many aspects of the immune response, such as phagocytosis and T-cell activation. Regulation of actin cytoskeleton remodeling depends on the activities of several proteins that coordinate events such as actin filament nucleation, elongation, capping, and cross-linking, in both space and time.

The functions of many cytoskeletal or actin-associated proteins have been well characterized, although the roles of some actin cytoskeleton proteins remain poorly understood. Among the less-characterized actin-associated proteins is leukocyte-specific protein 1 (LSP1). Initially described in B- and T-cells (Jongstra et al., 1988), LSP1 is also expressed in macrophages, neutrophils, endothelial cells, and various human myeloid and lymphoid cell lines (Kadiyala et al., 1990; Jongstra et al., 1994; Li et al., 1995; Palker et al., 1998; Jongstra-Bilen et al., 2000; Liu et al., 2005). Both mouse and human LSP1 are characterized by an acidic amino-terminal domain and a carboxy-terminal domain that is enriched with basic amino acids (Jongstra-Bilen et al., 1992). Alternative exon splicing generates four LSP1 isoforms, which differ by a 6–amino acid insert within the amino-terminal domain (Misener et al., 1994; Matsumoto et al. 1995b) or by a different sequence of the first 23 amino acids of the amino-terminal domain (Misener et al., 1994).

Similar to other actin cytoskeletal proteins such as gelsolin, LSP1 interacts with Ca^{2+} (Jongstra et al., 1988; Klein et al., 1989), although there is no evidence for a role of this interaction in the regulation of LSP1 function. Several studies showed that both human and mouse LSP1 are phosphorylated (Jongstra-Bilen et al., 1990; Matsumoto et al., 1993, 1995a; Carballo et al., 1996; Huang et al., 1997; Wu et al., 2007). In T- and B-cells, LSP1 is primarily phosphorylated by protein kinase C (PKC; Matsumoto et al., 1993, 1995a; Carballo et al., 1996), whereas in neutrophils, LSP1 is phosphorylated by

mitogen-activated protein (MAP) kinase–activated protein kinase 2 (MK2) after treatment with the chemoattractant formyl-methionyl-leucyl-phenylalanine (fMLP; Huang *et al.*, 1997; Wu *et al.*, 2007). Biochemical assays showed that phorbol 12-myristate 13-acetate–induced phosphorylation (PKC dependent) of LSP1 decreases its association with the plasma membrane (Matsumoto *et al.*, 1995a) and the actin cytoskeleton (Miyoshi *et al.*, 2001). However, others reported that phosphorylated, but not unphosphorylated, LSP1 primarily colocalizes with actin at the leading edge of fMLP-treated neutrophils (MK2-dependent phosphorylation; Wu *et al.*, 2007). Although the binding of LSP1 was not analyzed by Wu *et al.* (2007), colocalization data suggested that phosphorylated LSP1 preferentially associated with the actin cytoskeleton. Thus it is plausible that LSP1 has multiple phosphorylation states (generated by different kinases), which regulate its ability to link the plasma membrane to the underlying actin cytoskeleton. The importance of the interaction between kinases and LSP1 is further supported by the observation that LSP1 targets proteins of the ERK/MAP kinase pathway to the actin cytoskeleton (Harrison *et al.*, 2004).

LSP1 interacts with F-actin via villin headpiece–like sequences (KRYK and KYEK) located within their 30 carboxy-terminal amino acids (Klein *et al.*, 1990; Zhang *et al.*, 2001; Wong *et al.*, 2003). Furthermore, human LSP1 has two additional, weaker F-actin–binding regions that are homologous to the caldesmon actin-binding site (Zhang *et al.*, 2000, 2001). The overexpression of LSP1 in a wide variety of cells has been reported to cause the formation of long, actin-rich surface projections (Howard *et al.*, 1998; Miyoshi *et al.*, 2001) that require the actin-binding activity of LSP1 (Zhang *et al.*, 2001). Such a cell type–independent effect on the architecture of the actin cytoskeleton suggests that LSP1 may regulate actin cytoskeleton remodeling as well as cell motility. Indeed, the overexpression of LSP1 in human melanoma cells impairs their motility (Howard *et al.*, 1998). U937 cells, which do not express LSP1, migrate at a slower speed after overexpression of LSP1 (Li *et al.*, 2000). Moreover, neutrophils isolated from patients affected by neutrophil actin dysfunction, a syndrome characterized by recurrent infections, are characterized by the overexpression of LSP1 and exhibit a slower motility than normal neutrophils (Coates *et al.*, 1991; Howard *et al.*, 1994). Consistent with these observations, LSP1-deficient neutrophils migrate faster than wild-type cells in fMLP and KC gradients (Jongstra-Bilen *et al.*, 2000). These observations led to the hypothesis that LSP1 is a negative regulator of cell motility.

The role of LSP1 in the regulation of cell motility is likely to be more complex, as suggested by other investigations showing that LSP1-deficient neutrophils are slower and form fewer and smaller lamellipodia than control cells (Hannigan *et al.*, 2001). Moreover, the expression of LSP1 at physiological levels in U937 cells enhances, rather than impairs, cell motility (Li *et al.*, 2000). In this context, it must be taken into account that the substratum influences cellular responses to changes in LSP1 expression levels, as indicated by the observation that LSP1-deficient neutrophils migrate faster than control cells on fibrinogen but not fibronectin substrate (Wang *et al.*, 2002). Not surprisingly, LSP1-deficient neutrophils adhere better to both fibrinogen and intercellular adhesion molecule 1 than to fibronectin (Wang *et al.*, 2002).

In the present study, we characterized the function of LSP1 in the context of Fcγ receptor–mediated phagocytosis. LSP1 localized to nascent phagocytic cups during Fcγ receptor–mediated phagocytosis, where it displayed the same spatial and temporal distribution as actin filaments. Down-regulation of LSP1 severely reduced phagocytic activity of macrophages, clearly indicating a crucial role for this protein in Fcγ receptor–mediated phagocytosis. Furthermore, we demonstrated that LSP1 directly interacts with the SH3 domain of the molecular motor myosin1e and that both LSP1–myosin1e and LSP1–actin interactions are important for efficient Fcγ receptor–mediated phagocytosis.

RESULTS

LSP1 accumulates at sites of actin cytoskeleton remodeling around nascent phagosomes

To determine whether LSP1 plays a role in actin-dependent events associated with Fcγ receptor–mediated phagocytosis, we analyzed its spatial and temporal distribution during the internalization of opsonized beads. To this end, we generated two rabbit polyclonal antibodies that detected the last 16 carboxy-terminal amino acids of murine LSP1 (designated as polyclonal Cterm) or a peptide covering the central part of the amino terminus of LSP1 (polyclonal 2A). These peptide sequences were chosen because they are common to all known LSP1 isoforms. The polyclonal Cterm antibody reacted against a protein of the expected molecular size when tested with cytosolic lysates from J774 macrophages (50–52 kDa; Supplemental Figure S1), indicating that it is a reliable tool for analyzing the subcellular distribution of LSP1. The polyclonal 2A antibody also reacted against LSP1 (as well as green fluorescent protein [GFP]-tagged LSP1 that had been expressed in NIH-3T3 fibroblasts; Supplemental Figure S1), although it recognized an additional protein of ~25 kDa, making it suitable only for Western blotting analyses.

The distribution of LSP1 was then examined in macrophages 5 min after triggering the phagocytosis of opsonized beads. Within this time frame, the accumulation of actin, a distinctive feature of the phagocytic process, was observed at sites of bead internalization (Figure 1A). LSP1 was also localized to sites of internalization (Figure 1A), where its spatial distribution closely resembled that of actin. These findings suggest that LSP1 is involved in actin cytoskeleton remodeling during Fcγ receptor–mediated phagocytosis.

To corroborate these findings, we analyzed the dynamics of LSP1 in macrophages during phagosome formation. For this purpose, we engineered fluorescent variants of LSP1 by tagging it with red fluorescent protein (RFP) or GFP. Neither GFP nor RFP grossly affected the ability of LSP1 to associate with the actin cytoskeleton, as indicated by its colocalization with microfilaments and coprecipitation with actin from subcellular cytoskeletal fractions (Supplemental Figure S2). After the expression of LSP1-GFP in macrophages, we incubated these cells with opsonized beads and examined the spatial and temporal distribution of LSP1 at regular time intervals. As shown in Figure 1B, LSP1 initially accumulated at sites of bead–cell interaction. The accumulation of LSP1 at the phagocytic cups persisted as the phagocytosis proceeded, mirroring the previously described dynamics of actin (Araki *et al.*, 2003), finally disappearing as bead internalization was completed (Figure 1B; see also Supplemental Fig1B Video1). The same behavior of LSP1 was observed using macrophages expressing RFP-LSP1 during the uptake of opsonized sheep red blood cells (RBCs; Figure 1C and Supplemental Fig 1C Video2). Thus LSP1, similar to actin, transiently accumulates at forming phagosomes during the early stages of Fcγ receptor–mediated phagocytosis.

LSP1 is crucial for Fcγ receptor–mediated phagocytosis and requires association with the actin cytoskeleton

The observation that the spatial and temporal localization of LSP1 at nascent phagosomes mirrors that of actin prompted us to assess whether the recruitment of LSP1 at phagocytic cups is crucial for Fcγ receptor–mediated phagocytosis.
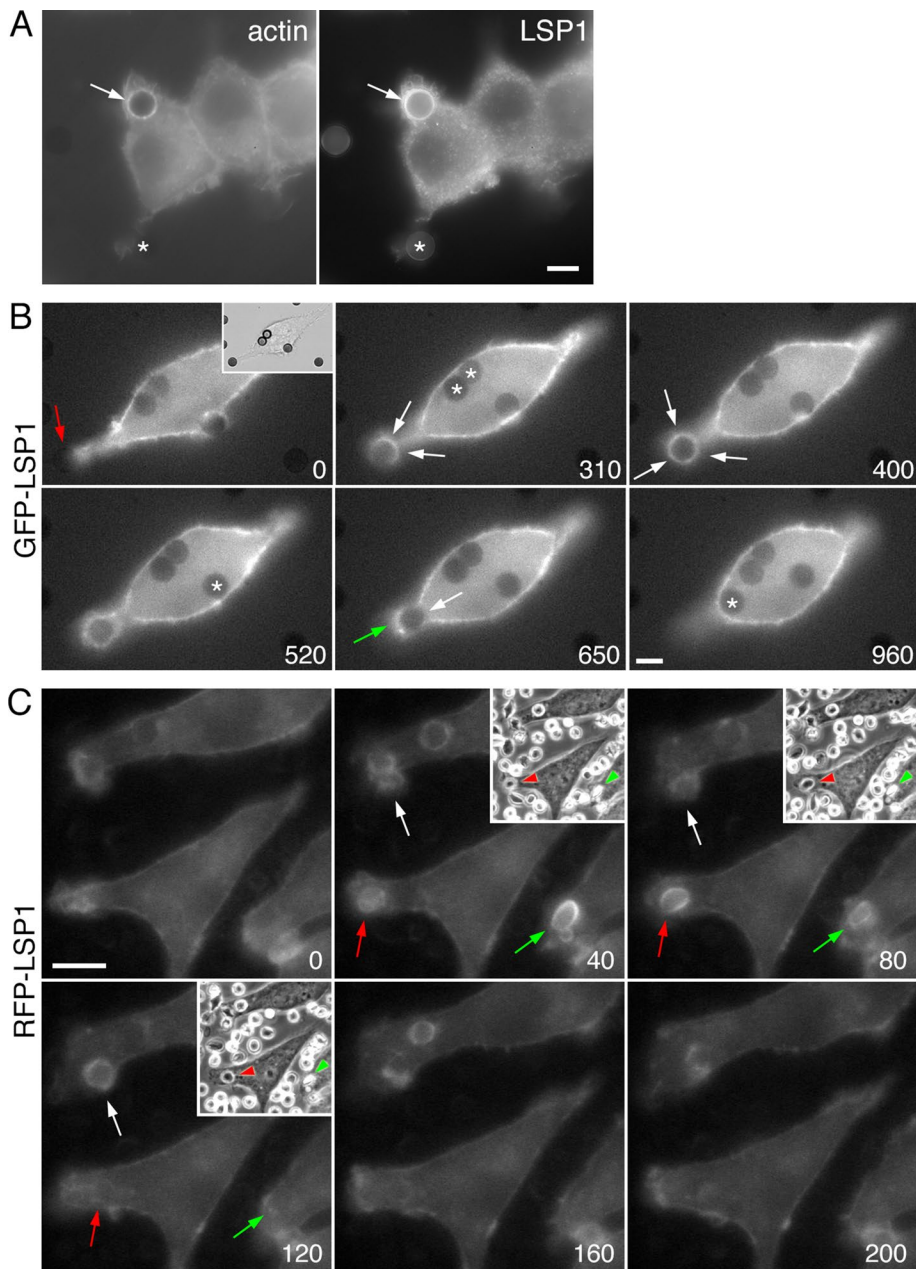
FIGURE 1: Localization and dynamics of LSP1 during Fcγ receptor–mediated phagocytosis. (A) Wide-field fluorescence images showing the spatial distribution of LSP1 in macrophages during Fcγ receptor–mediated phagocytosis. After incubation with opsonized beads for 5 min, actin concentrated around internalization sites (left, arrow), where LSP1 also accumulated (right, arrow). Conversely, beads that were not being internalized, and therefore negative for actin accumulation (left, asterisk), were also LSP1 negative (right, asterisk). Scale bar, 5 µm. (B, C) Macrophages expressing LSP1-GFP or RFP-LSP1 were incubated with opsonized beads and immediately analyzed by time-lapse fluorescence video microscopy. LSP1 accumulated at the sites of internalization within seconds of cell–bead (B, asterisks) interactions and remained at these locations as phagocytosis proceeded until the internalization process was complete (B and C, arrows). Note that LSP1 localization at the cell periphery is probably due to the interaction of LSP1 with the cortical actin cytoskeleton. Arrowheads in insets point to opsonized particles being taken up. Numbers represent elapsed time in seconds. Scale bar, 5 µm.

we validated in a previous study (Pust *et al.*, 2005). Two shRNAs, namely si316 and si755, reduced the level of LSP1 by 95 and 68%, respectively compared with its level in untreated control cells (Figure 2A). The scrambled shRNA had, as expected, no effect (Figure 2A). Subsequently, we examined Fcγ receptor–mediated phagocytosis in LSP1-deficient macrophages. In cells constitutively expressing the scrambled shRNA, formation of phagocytic cups around opsonized beads and localization of actin and LSP1 at these sites were unaffected (Figure 2B, right). In contrast, in cells expressing si316 or si755, the formation of mature phagocytic cups or the accumulation of LSP1 and actin at these sites was not observed (Figure 2B). These findings were further supported by the observation that the number of internalized RBCs per cells was clearly reduced in macrophages expressing si316 or si755 (Figure 2C). Moreover, scanning electron microscopy analysis showed that within 5 min after starting the phagocytic process, opsonized RBCs were almost completely surrounded by lamellipodia in control cells (Figure 2D), whereas the attachment of RBCs did not trigger formation of phagocytic cups in LSP1-deficient cells (Figure 2E).

As stated earlier, actin remodeling is fundamental for Fcγ receptor–mediated phagocytosis. Because LSP1 directly interacts with actin filaments, we sought to determine whether this interaction is required for the formation of phagocytic cups. For this purpose, we deleted the last 30 amino acids of LSP1, which have been shown to interact with actin filaments to generate LSP1-Δ30 (Klein *et al.*, 1990; Zhang *et al.*, 2001; Wong *et al.*, 2003; see Supplemental Figure S2, J–L). RFP-tagged LSP1-Δ30 was then transfected into LSP1-deficient cells (it was made refractory to the action of the shRNA si316 by introducing silent point mutations in the si316 target sequence). As expected, the LSP1-Δ30 mutant did not colocalize with the peripheral actin rim that was characteristic for these cells (Figure 3, A–C). Moreover, in all analyzed cells (~100 in three experiments), we could not detect the formation of actin-rich phagocytic cups around opsonized beads (Figure 3, D–F). This observation indicates that LSP1–actin interaction is essential for actin cytoskeleton remodeling at internalization sites. Overall we conclude that LSP1 is crucial for Fcγ receptor–mediated actin remodeling and phagocytosis.

To test this hypothesis, we down-regulated LSP1 expression in macrophages by using short hairpin RNA (shRNA) technology. We selected six different shRNAs, each targeting a different region within LSP1 mRNA. As control, we used a scrambled sequence that

LSP1 directly associates with myosin1e in macrophages

Based on the foregoing results, it is reasonable to assume that LSP1 regulates one or more steps of Fcγ receptor signal transduction pathways (Sechi, 2004). We therefore sought to assess the
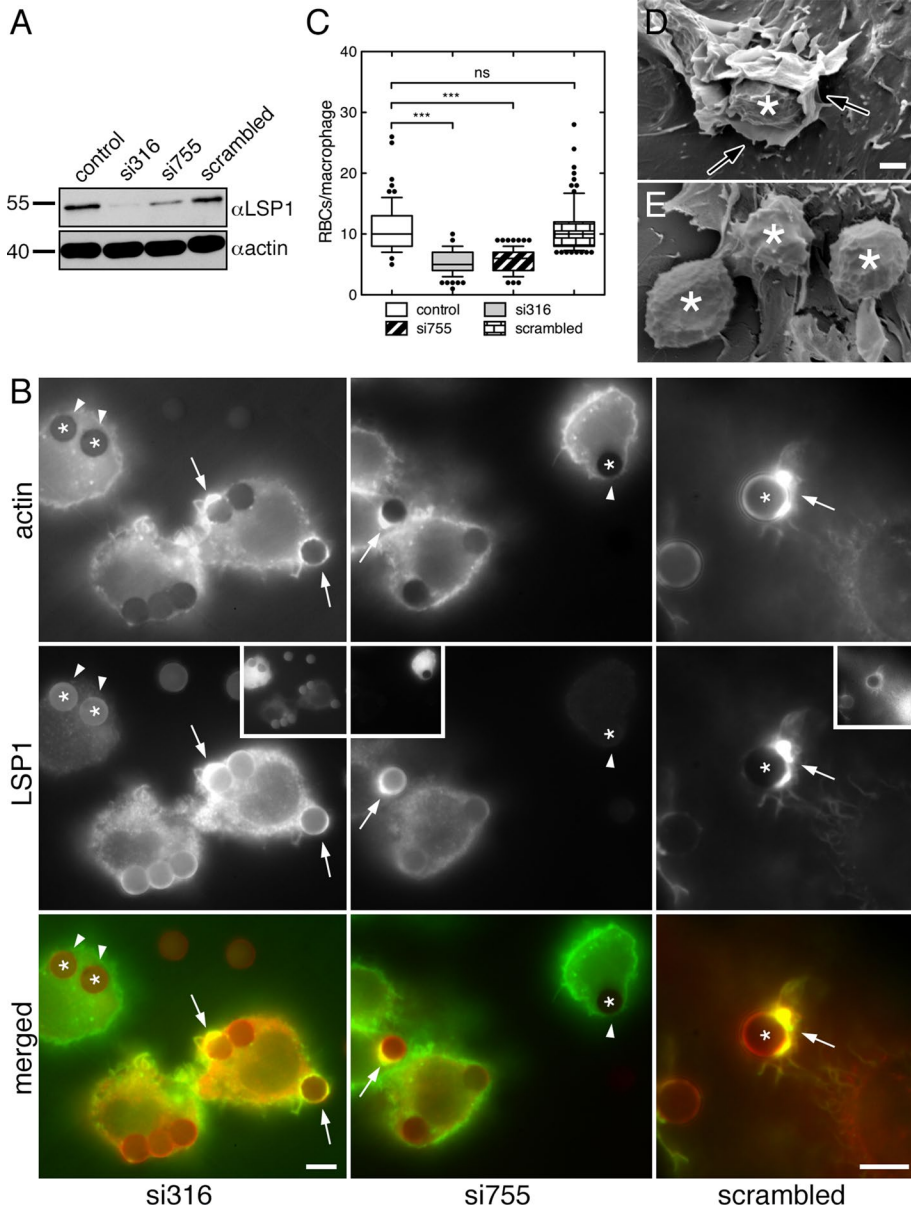
FIGURE 2: Down-regulation of LSP1 severely impairs Fcγ receptor–mediated phagocytosis. (A) shRNA-mediated down-regulation of LSP1 in macrophages. Cytosolic lysates from control untreated cells and cells stably transfected with LSP1-specific shRNAs (316 or 755) or a scrambled shRNA were analyzed for LSP1 expression by Western blotting. Compared with control cells, cells expressing si316 or si755 had much lower levels of LSP1. As expected, the scrambled control did not affect the expression of LSP1. Actin served as loading control. Numbers on the left indicate molecular weight markers in kilodaltons. (B) LSP1 deficiency greatly impairs actin remodeling during phagocytosis. In macrophages expressing si316 or si755 (see insets showing the GFP signal, which reflects shRNA expression), LSP1 levels were greatly reduced compared with control cells. At the sites of cell–bead contact, neither LSP1 nor actin accumulation could be detected (arrowheads; asterisks indicate the beads). This is in contrast with control cells or cells expressing the scrambled shRNA, in which LSP1 and actin colocalized at phagocytic cups (arrows). Scale bars, 5 μm (longer bar applies only to images on right). (C) Quantification of internalized RBCs in control and shRNA-expressing macrophages. Box-and-whiskers plots. The line in the middle of the box indicates the median, the top of the box indicates the 75th quartile, and the bottom of the box indicates the 25th quartile. Whiskers represent the 10th (lower) and 90th (upper) percentiles, respectively. Mann–Whitney U test, ***$p < 0.0001$; ns, nonsignificant difference. (D, E) LSP1 down-regulation impairs lamellipodium formation at Fcγ receptor internalization sites. Control macrophages (D) and LSP1-deficient macrophages (E) were incubated for 5 min at 37°C with opsonized RBCs (white asterisks), fixed, and processed for scanning electron microscopy. Control cells almost completely surrounded the opsonized targets with large lamellipodia (D, arrows). By

molecular mechanisms underlying the function of LSP1 in Fcγ receptor–mediated phagocytosis.

An obvious step toward this goal was to identify new binding partners of LSP1. To this end, we combined classical immunoprecipitation (IP) with mass spectrometry (MS) analysis. Using the C-term polyclonal antibody, we pulled down LSP1 from cytosolic lysates of macrophages and resolved the immunoprecipitate by SDS–PAGE. As compared with control IPs, LSP1 IPs contained several proteins ranging from 40 to 200 kDa (Figure 4A). The stimulation of macrophages with interferon γ (required to prime cells for phagocytosis) did not grossly change the binding properties of LSP1, as judged by the similar protein pattern found in LSP1 IPs (Figure 4A). Two of the proteins found in LSP1 IPs corresponded to unconventional myosin1c and myosin1e (Figure 4A), both of which are known to anchor the actin cytoskeleton to the plasma membrane (Woolner and Bement, 2009). The MS data were validated by Western blotting analysis using specific antibodies against myosin1c and myosin1e (Figure 4B). The specificity of the LSP1–myosin1e interaction was further confirmed by showing that myosin1e could not be coprecipitated from J774 lysates using a preimmune serum that did not bind to LSP1 (Supplemental Figure S4, A and B). Similarly, myosin1e could not be coprecipitated from NIH-3T3 lysates (which do not contain LSP1) using anti-LSP1 antibodies (Supplemental Figure S4C). Finally, to exclude nonspecific trapping in the actin meshwork, we added ATP in all immunoprecipitation steps to release myosins from actin filaments. As shown in Supplemental Figure S4D, the amount of myosin1e recovered in LSP1 IPs was not affected by the presence or absence of ATP, supporting the specificity of LSP1–myosin1e molecular complexes.

Closer inspection of LSP1 protein sequence revealed that it included sequences resembling class I (R/KxxPxxP; **K**SQ**P**TL**P** in LSP1) and atypical (RxxK; **R**SI**K** and **R**TP**K** in LSP1) SH3 domain–binding motifs (for details on these motifs, see Li, 2005). Because myosin1e has a SH3 domain at its carboxy terminus (Stöffler *et al.*, 1995), we speculated that LSP1 could directly interact with myosin1e. To test this hypothesis, we purified LSP1 and the SH3 domain of myosin1e

contrast, although LSP1-deficient cells were still able to bind the opsonized targets (white asterisks), they did not form lamellipodia around RBCs. Scale bar, 1 μm.
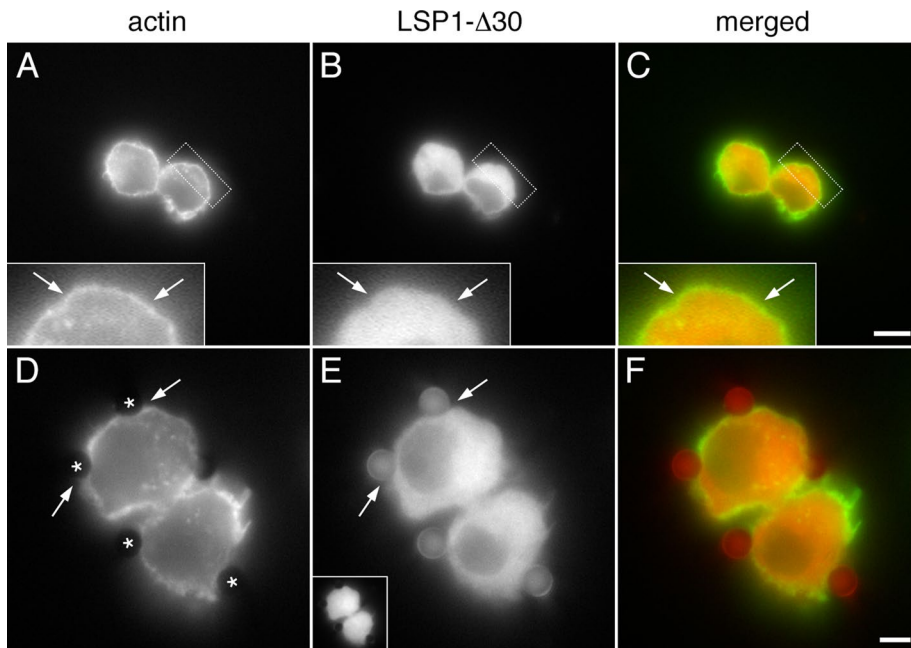
| actin | LSP1-Δ30 | merged |

FIGURE 3: The interaction of LSP1 with actin filaments is required for phagocytic cup formation. LSP1-deficient J774 macrophages expressing RFP-tagged LSP1-Δ30 were incubated with opsonized beads, fixed, and stained with Alexa 350–conjugated phalloidin. Note that, as expected, the LSP1-Δ30 did not colocalize with the actin rim at the periphery of J774 cells (A–C; arrows in insets). Moreover, cells expressing LSP1-Δ30 (D–F) did not accumulate actin and did not form phagocytic cups at the contact sites with opsonized beads (D, arrows ; asterisks indicate the beads), which were also devoid of LSP1-Δ30 (E, arrows). Inset in E shows the expression of shRNA 316. Scale bars, 10 μm (A–C), 5 μm (D–F).

(Supplemental Figure S3) and carried out an in vitro binding assay between LSP1 and glutathione *S*-transferase (GST)–tagged SH3 domain. As shown in Figure 4C, LSP1 was precipitated using beads coated with GST-SH3 but not with GST alone (Figure 4C), clearly demonstrating the direct association between LSP1 and myosin1e.

Next we sought to identify the binding site(s) for myosin1e within LSP1. Because the prolines within the class I motif R/KxxPxxP are crucial for interaction with SH3 domains (Li, 2005), we mutated the two prolines at positions 211 and 214 to alanine to generate LSP1 mut P>A. Moreover, we also replaced the arginines and the lysines within the two atypical SH3 domain–binding motifs with alanine (to generate LSP1 mut RK>A). After purification and in vitro binding assay with the SH3 domain of myosin1e, we found that the interaction of LSP1 with myosin1e was not affected by these mutations (Figure 4D). Therefore neither the class I motif nor the atypical motifs mediate the direct association between LSP1 and myosin1e.

By the systematic generation of deletion mutants, we found that the amino terminus of LSP1 is not required for its interaction with myosin1e (Figure 4, E and F; see also Supplemental Figure 4, E and F). In addition, a deletion mutant that roughly comprised one-third (Δ94) of the carboxy terminus did not bind to myosin1e (Figure 4F), whereas a mutant lacking the most 44 carboxy-terminal amino acids (Δ44) retained this binding activity (Figure 4F). Additional stepwise deletions using LSP1-Δ44 showed that the deletion of eight more amino acids abolished binding to the SH3 domain of myosin1e, suggesting that the amino acid sequence AGDMSKKS mediates LSP1–myosin1e interaction. Accordingly, an LSP1 mutant lacking only the sequence AGDMSKKS (ΔSBS for SH3-binding site) did not interact with the SH3 domain of myosin1e in vitro (Figure 4F). In this context, we tested whether two conserved tryptophan residues important for the binding activity of several SH3 domains

(Saksela and Permi, 2012) are required for the interaction of myosin1e with LSP1. To this end, we replaced the tryptophan residues in the hydrophobic groove of the SH3 domain with positively charged lysines (Tanaka *et al.*, 1995). These mutations inhibited the interaction of the SH3 domain of myosin1e with LSP1 (Supplemental Figure 4G), demonstrating that LSP1–myosin1e binding involves conserved residues known to be important for SH3 domain–ligand interactions.

To substantiate the function of the AGD-MSKKS sequence, we expressed the RFP-tagged LSP1-ΔSBS deletion mutant in LSP1-deficient macrophages. This mutant was made refractory to the action of the shRNA si316 by introducing silent point mutations in the si316 target sequence. As shown in Figure 4G (right), the deletion of the AGDM-SKKS sequence clearly reduced the ability of LSP1 to interact with myosin1e. Because the presence of myosin 1e in LSP1 IP could be due to the interaction with the residual endogenous LSP1 still present in LSP1-deficient macrophages, LSP1–myosin1e interaction was tested in NIH-3T3 cells, which do not express endogenous LSP1. As expected, LSP1–myosin1e interaction was fully functional also in this system, as judged by the recovery of myosin 1e in WT LSP1 IP. By contrast, in cells expressing LSP1-ΔSBS, the interaction of myosin1e with LSP1 was almost completely abolished (Figure 4G, left). These results corroborate the in vitro binding assays and demonstrate that the AGDMSKKS sequence is crucial for LSP1–myosin1e interaction.

Next we reasoned that if the interaction between LSP1 and myosin1e is crucial for Fcγ receptor–mediated phagocytosis, then macrophages expressing LSP1-ΔSBS should be impaired in their ability to take up opsonized RBCs. To test this hypothesis, we determined the number of RBCs taken up by cells expressing LSP1-ΔSBS and compared it with that of control and LSP1-deficient cells. The phagocytic function of cells expressing the LSP1-ΔSBS mutant was comparable to that of LSP1-deficient cells and much lower than that of control macrophages (Figure 4). Consistent with these data, actin, LSP1-ΔSBS, and myosin1e did not accumulate at the contact sites with opsonized beads (Figure 4I). Moreover, macrophages expressing the LSP1-ΔSBS mutant were unable to form phagocytic cups (Figure 4L). These findings clearly indicate that the LSP1–myosin1e complex plays a crucial role in Fcγ receptor–mediated phagocytosis.

LSP1 colocalizes with myosin1e at internalization sites during Fcγ receptor–mediated phagocytosis

Given that LSP1 is crucial for Fcγ receptor–mediated phagocytosis and interacts directly with myosin1e, it is plausible that the spatial and temporal localization at internalization sites of myosin1e should mirror that of LSP1.

To test our hypothesis, we generated macrophages that stably expressed GFP-myosin1e. After incubation with opsonized beads, cells were fixed, labeled with anti-LSP1 antibodies, and analyzed by fluorescence microscopy. Consistent with the data in Figure 1, LSP1

specifically accumulated at forming phagosomes but was absent from beads that were already internalized (Figure 5A). As anticipated, myosin1e distribution reflected that of LSP1 (Figures 5A and 6). Moreover, myosin1e dynamics mirrored that of actin during phagocytosis (Figures 5B and 6 and Supplemental Video 4). Further evidence for the directed binding between LSP1 and myosin1e came from the observation that the spatial and temporal distribution of myosin1e highly correlated with that of LSP1. Both proteins specifically concentrated at sites of bead–cell interaction, where they remained for the duration of the phagocytic process (Figure 5C and Supplemental Fig 5C Video5).

Finally, we determined the effect of LSP1 down-regulation on the spatial and temporal localization of myosin1e. As shown in Figure 7, A and B, myosin1e did not concentrate at bead–cell contact sites, suggesting that LSP1 regulates myosin1e recruitment at these locations.

Overall these findings demonstrate the participation of LSP1–myosin1e bimolecular complexes in Fcγ receptor–mediated phagocytosis and suggest that LSP1–myosin1e interaction is initiated by the activation of Fcγ receptors at internalization sites.

DISCUSSION

The precise temporal and spatial regulation of actin cytoskeleton remodeling is fundamental for Fcγ receptor–driven phagocytosis. In the present study, we demonstrate that the spatial and temporal distribution of LSP1 during Fcγ receptor–driven phagocytosis mirrors that of actin and that LSP1 down-regulation severely impairs phagocytosis. Accordingly, LSP1–actin interactions are essential for actin cytoskeleton remodeling at internalization sites. We also demonstrate that LSP1 binds to the class I molecular motor myosin1e. LSP1, which interacts with the SH3 domain of myosin1e, colocalizes with myosin1e at nascent phagocytic cups, and the dynamics of LSP1 and myosin1e at these locations reflects that of actin. Furthermore, the inhibition of LSP1–myosin1e interactions profoundly impairs phagocytosis. Thus the LSP1–myosin1e bimolecular complex plays a pivotal role in the regulation of actin cytoskeleton remodeling during Fcγ receptor–driven phagocytosis.

Studies on neutrophils and myeloid and lymphoid cell lines show that LSP1 regulates cell motility in a concentration-dependent manner (Li *et al.* 2000; Hannigan *et al.*, 2001; Jongstra-Bilen *et al.*, 2000; Wang *et al.*, 2002). Moreover, LSP1 overexpression causes the formation of actin-rich projections (Howard *et al.*, 1994, 1998; Miyoshi *et al.*, 2001). Therefore, LSP1 may control the remodeling of the actin cytoskeleton that supports lamellipodia formation by binding directly to actin filaments. Similarly, LSP1 could support the formation of lamellipodia at nascent phagocytic cups that progressively surround the particle being internalized (Figure 7C). In support of this hypothesis, we show that LSP1 localization and dynamics at such locations mirror those of actin and that the formation of lamellipodia around opsonized RBCs is severely impaired in LSP1-deficient cells. At present, we cannot exclude the possibility that LSP1 also regulates actin polymerization at forming phagocytic cups, although in vitro biochemical analyses seem to rule out a direct role for this protein in the regulation of actin polymerization kinetics (Jongstra-Bilen *et al.*, 1992).

Two of the earliest events after Fcγ receptor engagement include a wave of protein phosphorylation and an increase of free cytosolic Ca^{2+} (Sechi, 2004). The increase of Ca^{2+} levels directly affects the function of some cytoskeletal proteins, such as gelsolin, thus contributing to actin remodeling at the internalization sites. Of interest, LSP1 is believed to bind to Ca^{2+} (Jongstra *et al.*, 1988; Klein *et al.*, 1989), suggesting that its function and subcellular localization at

nascent phagosomes could be regulated by Ca^{2+} signaling. A second facet to be taken into account is the phosphorylation of LSP1. It has been shown that at least two kinases, MK2 and PKC, phosphorylate multiple serine residues within this protein (Matsumoto *et al.*, 1995a,b; Carballo *et al.*, 1996; Huang *et al.*, 1997; Wu *et al.*, 2007). Given both the role of some PKC isoforms in Fcγ receptor–driven phagocytosis (Larsen *et al.*, 2000, 2002; Mansfield *et al.*, 2000) and the observation that PKC-driven phosphorylation of LSP1 influences its membrane localization (Matsumoto *et al.*, 1995a), it is reasonable that kinase signaling also regulates LSP1 function during Fcγ receptor–driven phagocytosis.

Although actin cytoskeleton remodeling plays a fundamental role in Fcγ receptor–driven phagocytosis, it is, on its own, insufficient if it is not temporally and spatially coupled with localized contractile activity and lipid transport. The contractile activity is primarily due to myosin II, as indicated by the observation that its inhibition blocks phagocytosis (Araki *et al.*, 2003). Class I myosins seem not to be greatly involved in the contractile activity at phagocytic cups, but they are required for supporting the extension of pseudopodia around opsonized particles (Cox *et al.*, 2002; Dart *et al.*, 2012), possibly by delivering lipids to the forming phagocytic cups. Taking together the ability of myosin1e to interact with acidic phospholipids (Feeser *et al.*, 2010) and the present observation that the temporal and spatial distribution of myosin1e at phagocytic cups mirrors that of actin, we propose that one of the roles of myosin1e in this process is to transport along newly formed actin filaments the vesicles required for supporting membrane extension around opsonized targets. Furthermore, taking into account the ability of myosin1e to bind to key promoters of actin assembly, such as WIP and N-WASP (Cheng *et al.*, 2012), and its proposed role in the turnover of lamellipodia and invadosomes (Gupta *et al.*, 2013; Ouderkirk *et al.*, 2014), it is feasible that myosin1e also regulates actin assembly at nascent phagocytic cups (Figure 7C). In this context, the observations that pseudopodia formation around opsonized particles is severely impaired in both LSP1-deficient cells and in cells expressing the LSP1-ΔSBS mutant suggest that LSP1 contributes to the localization of myosin1e at internalization sites, where LSP1 and myosin1e work in concert to regulate actin cytoskeleton assembly and remodeling and membrane extension during Fcγ receptor–driven phagocytosis (Figure 7C).

At variance with the classical interaction of SH3 domains with ligands containing proline-rich motifs, we showed here that a novel noncanonical amino acid sequence is involved in the interaction between LSP1 and the SH3 domain of myosin1e. Of interest, mutation of conserved tryptophan residues within the hydrophobic pocket of the myosin1e SH3 domain, which interacts with proline-rich domains (Krendel *et al.*, 2007), abolishes its interaction with LSP1, indicating that they are crucial for this novel interaction. As to the structural basis of the interaction(s) between the noncanonical SH3 domain–binding site of LSP1 and the SH3 domain of myosin1e, the lack of information about LSP1 protein folding makes it difficult to put forward any precise hypothesis. It is noteworthy, however, that positively charged amino acids are important for binding to SH3 domains (Li, 2005, and references therein) and that the noncanonical sequence AGDMSKKS contains two positively charged amino acids and has an overall positive charge at pH 7.0. It is therefore reasonable to hypothesize that electrostatic interactions mediate the binding of LSP1 to myosin1e. It may also be possible that the interaction of LSP1 with the SH3 domain of myosin1e involves tertiary interactions between complementary interfaces, as shown for other ligand–SH3 domain associations (Li, 2005, and references therein). In this context, the noncanonical
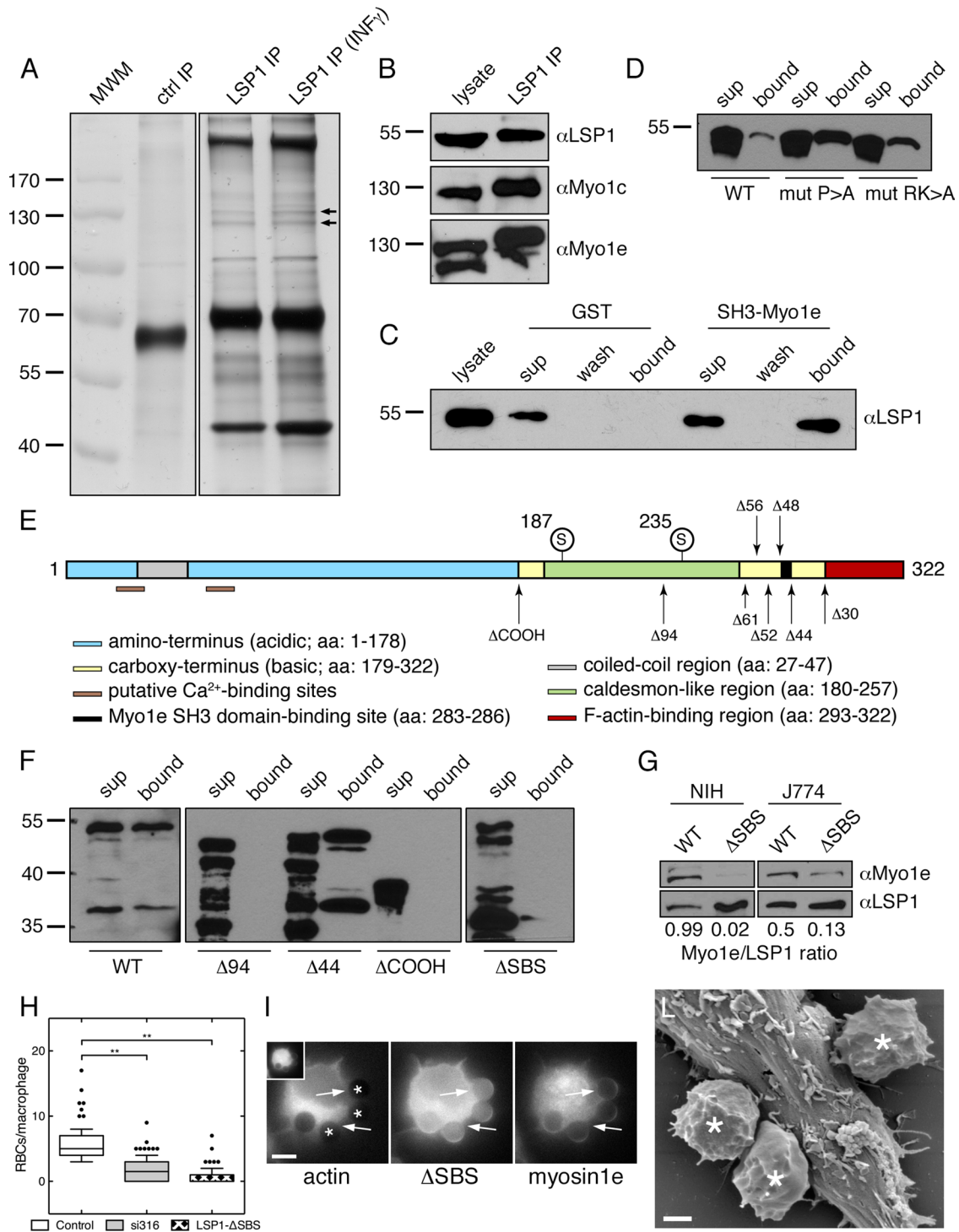
FIGURE 4: Characterization of the direct binding between LSP1 and myosin1e. (A, B) LSP1 forms protein complex(es) with myosin1c and myosin1e in macrophages. (A) SDS–PAGE gel (after silver staining), showing proteins that coprecipitated with LSP1 from J774 cytosolic lysates. Control IP (ctrl IP) was done using beads coated with BSA. Arrows indicate the expected positions of myosin 1c (lower arrow) and myosin1e (upper arrow). MWM, molecular weight markers (in kilodaltons). (B) Western blotting showing the presence of myosin1c and myosin1e in both cytosolic lysates and LSP1 immunoprecipitates (LSP1 IP). Numbers on the left indicate molecular weight markers in kilodaltons. (C) LSP1 directly interacts with the SH3 domain of myosin1e. Purified LSP1 was incubated with either GST or GST-SH3. After incubating with glutathione beads (bound to GST), the presence of LSP1 in the supernatant (after centrifugation of beads), wash (after third washing step), and eluate (bound to beads) fractions was tested by Western blotting. LSP1 bound to GST-SH3 but not to GST, indicating a direct LSP1–SH3 domain interaction. J774 cytosolic lysate (lysate) served as positive control. Number on the left indicates molecular weight marker in kilodaltons. (D) Class I and atypical SH3 domain–binding sequences within LSP1 are dispensable for its interaction with the SH3 domain of myosin1e. The replacement of proline residues with alanine within the class I motif R/KxxPxxP (mut P>A) or arginine and lysine residues

sequence AGDMSKKS may not directly contribute to the interaction with the SH3 domain but instead participate in the formation of the complementary interface within LSP1. In addition to structural determinants of LSP1–myosin1e interaction, its strength and contextual specificity, as well as its potential competition with classical SH3 ligands, should be the focus of future biochemical and crystallographic studies.

We anticipate that the present findings will assist in a better understanding of the molecular basis of Fcγ receptor–driven phagocytosis and the underlying phenomenon of innate immunity. They will also be instrumental to characterize precisely the inhibition/impairment of phagocytosis induced by some pathogens, such as *Yersinia* species (Sechi, 2004), and develop pharmacological tools to counteract it. Future studies should also be aimed at precisely defining the role(s) and functional coordination of LSP1 and myosin1e in other biological processes, such as cell motility, that require localized remodeling of the actin cytoskeleton.

MATERIALS AND METHODS
Cloning of LSP1 and myosin1e constructs
The open reading frame of mouse LSP1 was obtained from the Deutsches Ressourcenzentrum für Genomforschung (Germany). LSP1 full length and LSP1-Δ30 were cloned into pWPXL (from D. Trono, École Polytechnique Fédérale de Lausanne, Lausanne, Switzerland) using *Bam*HI and *Mlu*I (for primers, see Supplemental Table I) to obtain LSP1-GFP and LSP1-Δ30-GFP, respectively. shRNA-refractory LSP1 mutants were generated by introducing silent point mutations in the si316 sequence by site-directed mutagenesis (Supplemental Table I) using QuikChange Primer Design (Agilent Technologies, Santa Clara, CA). The following bases (in bold) were mutated in the si316 sequence: GG**C**AC**C**GA**G**CC**T**TC**C**CA**G**A. LSP1-ΔSBS-GFP was generated by overlap extension PCR using pWPXL-LSP1-GFP as the template. LSP1 full-length and LSP1-ΔSBS were cloned into pGEX-4T1 using *Bam*HI and *Xho*I. All LSP1 truncated variants were generated using pGEX-4T1-LSP1 full-length as the template by inserting a stop codon at the desired location by site-directed mutagenesis. To generate RFP-LSP1-ΔSBS, GFP was excised from pWPXL-GFP and replaced with RFP (kindly provided by R. Tsien, University of California, San Diego). Afterward, LSP1-ΔSBS was amplified from pGEX-4T1-LSP1-ΔSBS and cloned into pWPXL-RFP previously digested with *Bsp*119I and *Bam*HI. RFP-LSP1 full length was generated by excising LSP1 from pMSCV-GFP-LSP1 with *Bsp*119I and *Bam*HI and cloning into the same restriction sites of pWPXL-RFP. Myosin1e SH3 domain (cDNA kindly provided by M. Bähler, Westfälische Wilhelms Universität Münster, Münster, Germany) was cloned into pGEX-4T using *Bam*HI and *Xho*I, whereas full-length myosin1e (cDNA kindly provided by M. Bähler) was cloned into pWPXL-GFP using *Mss*I and *Bsp*119I. All constructs were verified by DNA sequencing.

Cell culture
NIH-3T3 mouse fibroblasts (CRL 1658; American Type Culture Collection [ATCC, Manassas, VA]) and J774 mouse macrophages (TIB 67; ATCC) were grown in DMEM supplemented with 10% fetal calf serum (FCS), 4 mM L-glutamine, 100 μg/ml streptomycin, and 100 U/ml penicillin. The packaging cell line 293T (CRL 11268; ATCC) was grown in DMEM high glucose supplemented with 10% FCS, 2 mM L-glutamine, 1 mM sodium pyruvate, 100 μg/ml streptomycin, and 100 U/ml penicillin. All cell lines were grown at 37°C and 5% CO_2.

Production of retroviruses, lentiviruses, and cell infection
Constitutive gene expression or down-regulation was obtained by virus-mediated gene delivery. For constitutive gene expression, pWPXL-based constructs were cotransfected with the psPAX2 (carrying the gag and pol viral genes; kindly provided by D. Trono) and pMD2.G (carrying the envelope viral gene) into 293T packaging cells by using a calcium phosphate transfection procedure. The same procedure was applied for the down-regulation of LSP1, using the silencing vector pLVTHM_si316, pLVTHM_si755 or pLVTHM_siScrbl, the packaging vector pCMV-dR8.74 (carrying the gag and pol viral genes; kindly provided by D. Trono), and pMD2.G. In both cases, the cell medium containing the retroviral particles was collected 2 d later and used to infect NIH-3T3 or J774 cells. Infection was done by mixing the viral supernatant with fresh cell medium (1:1 ratio) and 8 μg/ml Polybrene, followed by centrifugation at $1200 \times g$ for 2 h at 24°C. Infected cells were selected by fluorescence-activated cell sorting according to high levels for all silencing vectors and middle to high levels for all expression vectors.

Protein production and purification
GST-tagged LSP1 variants and GST-tagged SH3 domain of myosin1e were produced in *Escherichia coli* BL21 transformed with pGex4T1 vectors (see earlier description). After reaching an optical density OD_{600} of 0.5–0.7, bacterial cultures were treated with 1 mM isopropyl-β-D-thiogalactoside (IPTG; 4 h, 37°C) to induce protein expression. IPTG-stimulated bacteria were centrifuged and the pellets stored at −80°C until use.

Proteins were isolated from bacterial pellets after incubation with 200 mg/ml lysozyme (in ice-cold TNE buffer; 20 mM Tris, pH 8.0, 150 mM NaCl, 1 mM EDTA, 5 mM dithiothreitol, 1 mM Pefabloc, 1.4 μg/ml Trasyol) for 30 min on ice. After sonication (four times, 20 pulses), protein samples were clarified by centrifugation at $10,000 \times g$ for 30 min at 4°C. Afterward, supernatants were incubated with glutathione agarose 4B beads (Macherey-Nagel, Düren, Germany) for 1 h at 4°C with constant mixing. After centrifugation at $500 \times g$ for 2 min at 4°C, supernatants were discarded and the beads washed three times with ice-cold phosphate-buffered saline (PBS). Next beads were resuspended in 1 ml of PBS, transferred to a chromatography column (Poly-prep; Bio-Rad, Hercules, CA), and washed

---

within the two atypical SH3 domain–binding motifs of LSP1 (mut RK>A) did not grossly affect the ability of LSP1 to interact with the SH3 domain of myosin1e. Number on the left indicates molecular weight marker in kilodaltons. (E) Schematic representation of LSP1 domain structure and binding sites. (F, G) Deletion of the novel SH3 domain–binding (SBS) site of LSP1 severely impairs its ability to interact with myosin1e. (F) In vitro binding assays between LSP1 deletion mutants and the SH3 domain of myosin1e. Numbers on the left indicate molecular weight markers in kilodaltons. Sup, input; bound, IPs. (G) Pull-down assays from NIH-3T3 and J774 cell lysates. Numbers at the bottom indicate the myosin1e/LSP1 ratio as determined by densitometry analysis using ImageJ. (H) Inhibition of LSP1-myosin1e interaction inhibits Fcγ receptor–driven phagocytosis. Phagocytosis of RBCs was quantified in LSP1-deficient cells expressing the LSP1-ΔSBS mutant. Mann–Whitney *U* test, **p < 0.0001. (I) Immunofluorescence labeling, showing the lack of actin, LSP1-ΔSBS, and myosin1e accumulation at the contact sites (arrows) with opsonized beads (asterisks). Inset, si316 expression. Scale bar, 5 μm. (L) J774 cells expressing LSP1-ΔSBS were still able to bind opsonized RBCs (white asterisks), but they did not form lamellipodia around them. Scale bar, 1 μm.
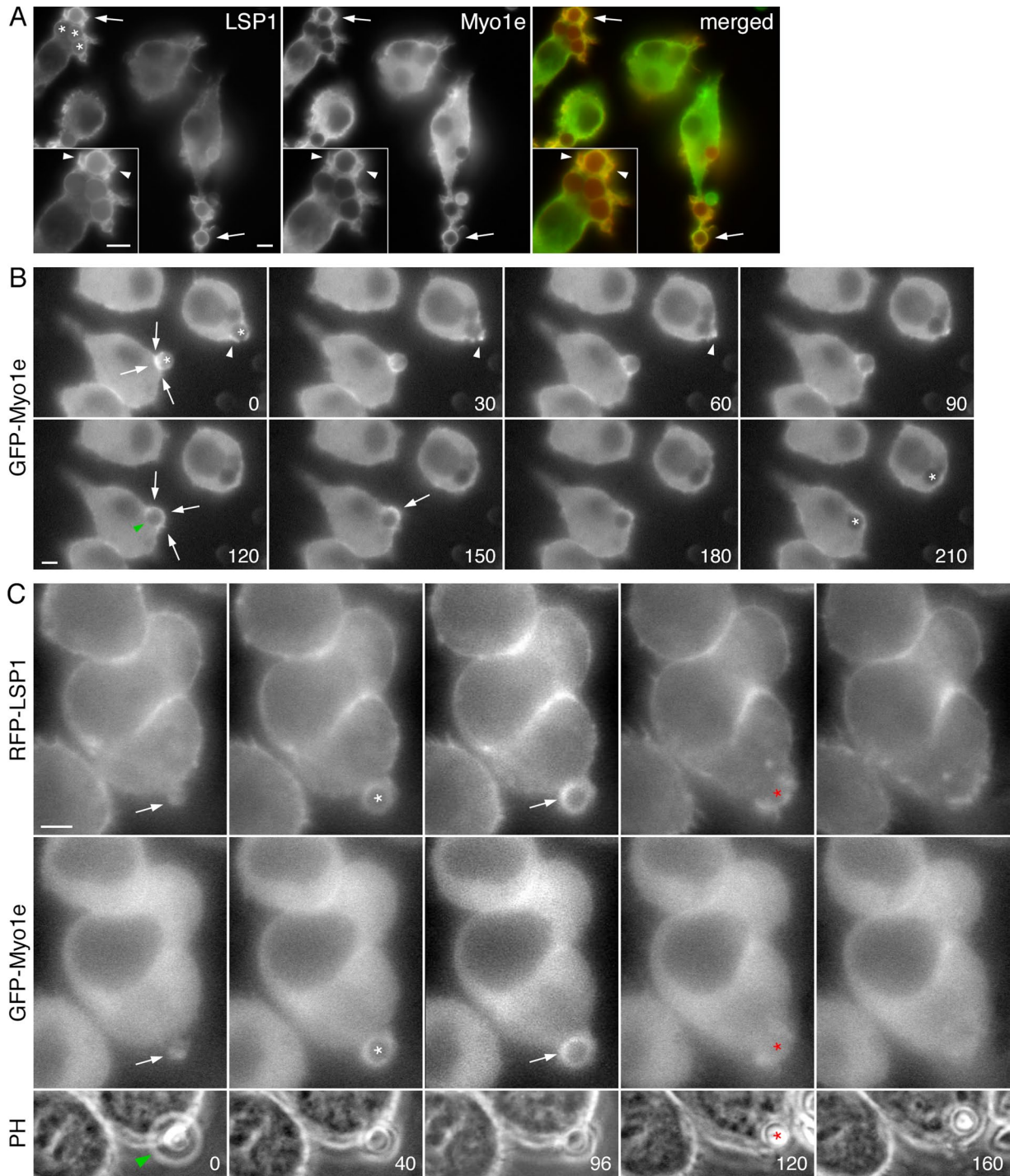
FIGURE 5: LSP1 and myosin1e have the same spatial and temporal distribution during Fcγ receptor–mediated phagocytosis. (A) LSP1 and myosin1e colocalize at phagocytic cups. After incubation with opsonized beads, macrophages stably transfected with GFP-myosin1e were fixed and labeled with anti-LSP1 antibodies. The levels of both proteins (arrows) are highest around beads (asterisks) at internalization sites. Scale bars, 5 μm. (B) Dynamics of myosin1e during Fcγ receptor–mediated phagocytosis. J774 cells expressing GFP-myosin1e were incubated with opsonized beads and immediately analyzed by time-lapse fluorescence video microscopy (Supplemental Fig5B Video3). Myosin1e initially accumulated at the proximal side of a bead (arrows; asterisks indicate beads). As phagocytosis proceeded, myosin1e accumulation could be observed on the lateral sides of a bead and finally on its distal portion (arrows). The green arrowhead points to the proximal, already internalized, portion of a bead devoid of myosin1e. (C) Dynamics of myosin1e and LSP1 during Fcγ receptor–mediated phagocytosis. Cells expressing both GFP-myosin1e and RFP-LSP1 were incubated with opsonized beads and immediately analyzed by time-lapse fluorescence video microscopy. In agreement with the data in A and B, the proteins showed similar dynamics throughout particle internalization (arrows; asterisks indicate beads). The green arrowhead points to the bead in the corresponding phase contrast images. Numbers represent elapsed time in seconds. Scale bar, 5 μm.
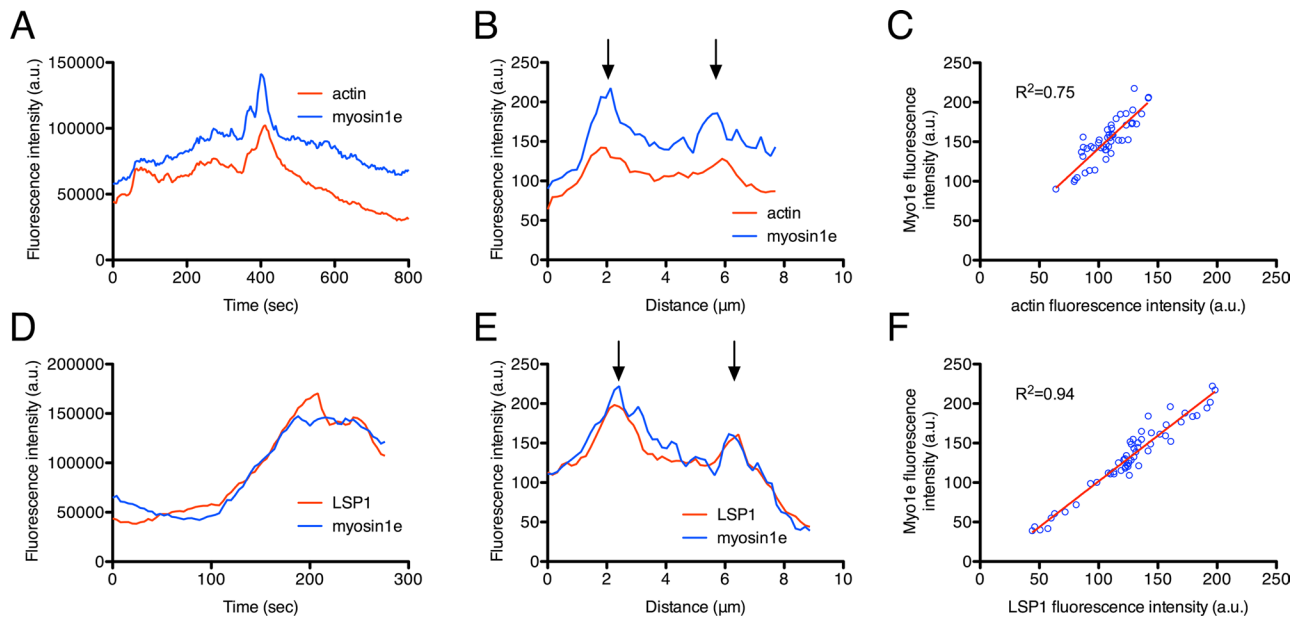
FIGURE 6: Fluorescence intensity analysis of LSP1, actin, and myosin1e during Fcγ receptor–mediated phagocytosis. (A, B, D, E) Plots showing the distribution of actin and myosin1e (A) or LSP1 and myosin1e (D) during phagocytosis in live cells. (B, E) Accumulation of myosin1e and actin (B) or LSP1 and myosin1e (E) around phagocytic cups in fixed cells. Arrows in B and E indicate the maximum intensity of LSP1 and myosin1e corresponding to the bead edges. (C, F) Plots for myosin1e-actin (C) and LSP1-myosin1e (F) pairs, showing a high correlation for the intensity values of these proteins at phagocytic cups.

with GST washing buffer (100 mM Tris/HCl, pH 8.0, 120 mM NaCl). GST-tagged proteins were eluted with 300 μl (three times, 5-min incubation at 4°C) of GST elution buffer (20 mM glutathione in GST washing buffer).

To remove the GST tag, bead-bound proteins were incubated with 1 U/μl thrombin in PBS (supplemented with protease inhibitors) for 1 h at 37°C. The mix was then transferred to a chromatography column and the flowthrough collected. Thrombin was removed from the protein preparations after the incubation with benzamidine Sepharose beads (GE Healthcare, Chalfon St Giles, United Kingdom) for 2 h at 4°C. A fresh chromatography column was used to remove thrombin. Proteins were divided into aliquots, flash frozen in liquid nitrogen, and stored at −80°C.

Immunoprecipitation and in vitro binding assay
For the identification of novel LSP1-binding proteins, LSP1 was immunoprecipitated from protein lysates of J774 cells using tosylactivated Dynal beads (Life Technologies, Carlsbad, CA) covalently coupled to the C-term anti-LSP1 antibody according to standard procedures. Control immunoprecipitations were done using beads covalently coupled to bovine serum albumin (BSA). Immunoprecipitates were resuspended in sample buffer and resolved by SDS–PAGE, and the protein bands were visualized by silver staining. Protein bands present in the LSP1 but not in the control immunoprecipitates were excised from the gel and identified by mass spectrometry at the GIGA proteomics facility of the University of Liège (Liège, Belgium). The mass spectrometry analysis was validated by probing LSP1 immunoprecipitates with the polyclonal antibodies Tü49 (anti-myosin1c) and Tü58 (anti-myosin1e; kindly provided by M. Bähler).

To determine the interaction of LSP1 variants with GST-tagged SH3 domain of myosin1e, 10 μl of glutathione agarose 4B beads was incubated with 4 μg of GST-SH3 and 4 μg of LSP1 proteins in pull-down buffer (20 mM 4-(2-hydroxyethyl)-1-piperazineethanesulfonic acid, pH 7.4, 50 mM NaCl, 1.5 mM EDTA, 0.1% NP-40, supplemented with protease inhibitors) for 3 h at 4°C (with constant mixing). Control binding assays were done using GST instead of GST-SH3. The incubation mix was then centrifuged at $500 \times g$ for 2 min at 4°C, the supernatant collected, and the beads washed three times with pull-down buffer (containing 150 mM NaCl and protease inhibitors). Finally, beads were resuspended in sample buffer, and the binding of LSP1 variants to the SH3 domain of myosin1e was determined by Western blotting with anti-LSP1 antibodies.

Determination of LSP1-actin interaction by Triton-soluble/insoluble extraction
The interaction of LSP1 variants with the actin cytoskeleton was determined as follows. Monolayers of NIH-3T3 cells expressing LSP1 variants were washed once with prewarmed (37°C) PBS. Cells were then lysed with cytoskeleton lysis buffer (CLB; 0.5% Triton X-100, 10 mM 1,4-piperazinediethanesulfonic acid, pH 7.4, 150 mM NaCl, 5 mM ethylene glycol tetraacetic acid [EGTA], 5 mM glucose, 5 mM magnesium chloride, supplemented with 0.5 mM sodium fluoride, 1 mM sodium orthovanadate, and protease inhibitor cocktail) for 10 min on ice. Afterward, the CLB (Triton-soluble or cytosolic fraction) was collected and clarified at $10,000 \times g$ for 10 min at 4°C. The cell monolayer was then washed twice with ice-cold CLB and incubated with RIPA buffer (50 mM Tris-HCl, pH 7.4, 1% NP-40, 0.1% SDS, 0.25% sodium deoxycholate, 150 mM NaCl, 5 mM EGTA, 3 mM phenylmethylsulfonyl fluoride, protease inhibitor cocktail, 1 mM sodium fluoride, and 1 mM sodium orthovanadate) for 15 min on ice. After the cells were scraped off, the RIPA buffer (Triton-insoluble or cytoskeletal fraction) was clarified at $12,000 \times g$ for 10 min at 4°C. Both fractions were probed with antibodies against LSP1 and actin (clone AC-74; Sigma-Aldrich, St. Louis, MO).
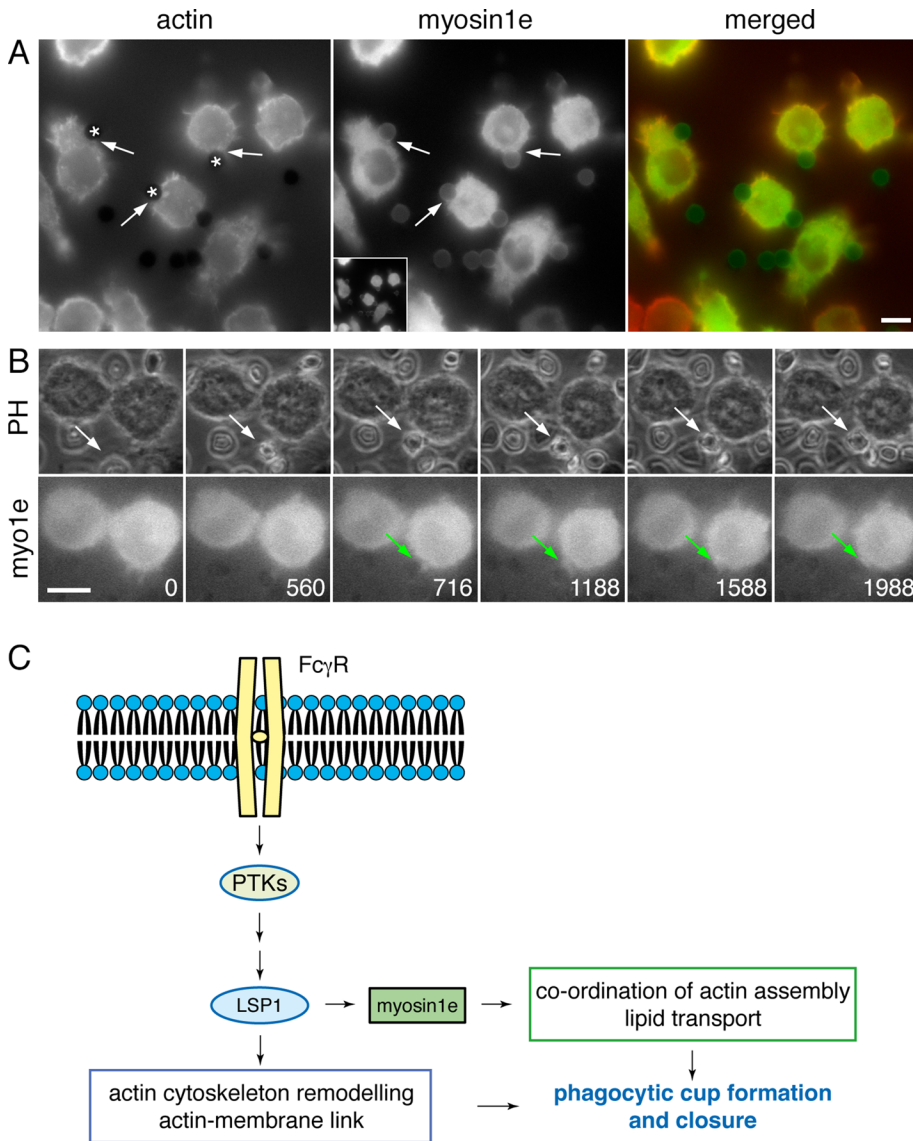
FIGURE 7: LSP1 deficiency impairs myosin1e accumulation at internalization sites. (A, B) After incubation with opsonized beads, LSP1-deficient J774 cells were fixed and labeled with Alexa 350–conjugated phalloidin and anti-myosin1e antibodies. Arrows point to the bead–cell contact sites and show the lack of actin and myosin1e accumulation at these locations. Asterisks indicate opsonized beads. In the merged image, actin and myosin1e are represented in red and green, respectively. Scale bar, 10 µm. (B) Dynamics of myosin1e Fcγ receptor–mediated phagocytosis in LSP1-deficient cells. Cells expressing GFP-myosin1e were incubated with opsonized RBCs and analyzed by time-lapse fluorescence video microscopy (Supplemental Fig7B Video6). In agreement with the data in A, myosin1e did not accumulate at the bead–cell contact site throughout the imaging time (white arrows point to RBCs, whereas green arrows highlight the lack of myosin1e accumulation at the RBC–cell interface). Numbers represent elapsed time in seconds. Scale bar, 10 µm. (C) Schematic model for the role of LSP1 and myosin1e during Fcγ receptor–mediated phagocytosis. After the engagement of Fcγ receptors, early events, including the activation of protein kinases (PTKs), will lead to the recruitment of LSP1, which, in turn, will interact with myosin1e at nascent phagocytic cups. At these locations, LSP1 and myosin1e will work in concert to coordinate actin assembly, lipid transport, and actin–membrane linkage, finally leading to phagocytic cup formation and closure.

Phagocytosis assay

The ability of J774 cells to take up opsonized sheep erythrocytes or magnetic beads was evaluated as described (Coppolino et al., 2001). Phagocytosis efficiency was determined by counting the number of internalized sheep RBCs per cell (in 80–85 cells). To avoid counting noninternalized RBCs, noninternalized RBCs were lysed by brief treatment (5 s) with distilled water before fixation with paraformaldehyde. For time-lapse imaging of phagocytosis, macrophages expressing fluorescent LSP1 or myosin1e (or both) were placed in a heating stage and overlaid with opsonized beads or RBCs. Pairs of phase contrast and fluorescence images were acquired every 2 or 5 s as described next.

Immunofluorescence labeling and video microscopy

Immunofluorescence labeling and video microscopy were done as described (Geese et al., 2002; Pust et al., 2005; Würflinger et al., 2011). Rabbit polyclonal antibodies against LSP1 were generated and affinity purified using the peptides 2A (92–108; KPEPRQQFWGNEGTAEG) and C-term (315–330; CHGKYEKVLVDEGSAP) by Pineda antibody service (Berlin, Germany). Myosin1e was detected using the rabbit polyclonal antibody Tü58 or ARP56601 (Aviva Systems Biology, San Diego, CA). The actin cytoskeleton was visualized using Alexa 594–, Alexa 488–, or Alexa 350–conjugated phalloidin (Life Technologies). Secondary antibodies were Alexa 594 or Alexa 488 anti-rabbit immunoglobulin G (Life Technologies). Coverslips were mounted in Prolong (Life Technologies). Images were acquired using an Axio Observer Z1 inverted microscope equipped with an Evolve electron-multiplying charge-coupled device camera driven by ZEN software (Carl Zeiss, Jena, Germany).

For live-cell imaging, phase contrast and epifluorescence images were acquired with an Axiovert 200 microscope (Carl Zeiss) using a Plan-Apochromat 100×/1.4 numerical aperture objective in combination with 1.6× or 2.5× Optovar optics. Imaging of RFP-LSP1 and GFP-myosin1e during phagocytosis was done using a Mac5000 filter wheel equipped with exciters for RFP and GFP and a double-bandpass filter cube. To reduce photobleaching of RFP and GFP, exposure time was kept as low as possible (maximum 500 ms) by using the on-chip multiplication amplification mode. To minimize the time offset between the acquisition of the RFP-LSP1 and GFP-myosin1e images, the image requiring the longer exposure time (i.e., GFP-myosin1e) was acquired first. Images were recorded with a cooled, backilluminated charge-coupled device camera (Cascade 512B; Photometrics, Tucson, AZ) driven by IPLab Spectrum software (Scanalytics, Fairfax, VA). When required, the brightness and contrast of the images were adjusted to improve clarity. Digital handling of the images was done using iVision (BioVision Technologies, Exton, PA), ImageJ, and Photoshop 8.0 (Adobe, San José, CA).

Scanning electron microscopy

For scanning electron microscopy analysis, samples were fixed with 3% glutaraldehyde (Agar Scientific, Standsted, United Kingdom) in Soerensen's phosphate buffer (Merck, Darmstadt, Germany) for 1 h at room temperature. After washing with Soerensen's phosphate buffer for 15 min, samples were dehydrated through a graded ethanol series. Drying of the samples was done in hexamethyldisilazane (Sigma-Aldrich) for 20 min at room temperature, followed by sputter coating with a 10-nm gold layer. Samples were examined with a digital scanning electron microscope (ESEM XL30 FEG; FEI, Hillsboro, OR) using a working distance of 8 mm and an acceleration voltage of 5 kV. Electron microscopy images were processed using Photoshop 8.0.

Statistical analysis

Graphs and statistical tests were done using Prism 5 (GraphPad Software, La Jolla, CA). Differences between sample pairs were analyzed using the two-tailed Mann–Whitney nonparametric U test. The null hypotheses (the two samples have the same median values, that is, they are not different) were rejected when $p > 0.5$.

REFERENCES

Araki N, Hatae T, Furukawa A, Swanson JA (2003). Phosphoinositide-3-kinase-independent contractile activities associated with Fcgamma-receptor-mediated phagocytosis and macropinocytosis in macrophages. J Cell Sci 116, 247–257.

Carballo E, Colomer D, Vives-Corrons JL, Blackshear PJ, Gil J (1996). Characterization and purification of a protein kinase C substrate in human B cells. Identification as lymphocyte-specific protein 1 (LSP1). J Immunol 156, 1709–1713.

Cheng J, Grassart A, Drubin DG (2012). Myosin 1E coordinates actin assembly and cargo trafficking during clathrin-mediated endocytosis. Mol Biol Cell 23, 2891–2904.

Coates TD, Torkildson JC, Torres M, Church JA, Howard TH (1991). An inherited defect of neutrophil motility and microfilamentous cytoskeleton associated with abnormalities in 47-Kd and 89-Kd proteins. Blood 78, 1338–1346.

Coppolino MG, Krause M, Hagendorff P, Monner DA, Trimble W, Grinstein S, Wehland J, Sechi AS (2001). Evidence for a molecular complex consisting of Fyb/SLAP, SLP-76, Nck, VASP and WASP that links the actin cytoskeleton to Fcgamma receptor signalling during phagocytosis. J Cell Sci 114, 4307–4318.

Cox D, Berg JS, Cammer M, Chinegwundoh JO, Dale BM, Cheney RE, Greenberg S (2002). Myosin X is a downstream effector of PI(3)K during phagocytosis. Nat Cell Biol 4, 469–477.

Dart AE, Tollis S, Bright MD, Frankel G, Endres RG (2012). The motor protein myosin 1G functions in FcgammaR-mediated phagocytosis. J Cell Sci 125, 6020–6029.

Feeser EA, Ignacio CM, Krendel M, Ostap EM (2010). Myo1e binds anionic phospholipids with high affinity. Biochemistry 49, 9353–9360.

Geese M, Loureiro JJ, Bear JE, Wehland J, Gertler FB, Sechi AS (2002). Contribution of Ena/VASP proteins to intracellular motility of listeria requires phosphorylation and proline-rich core but not F-actin binding or multimerization. Mol Biol Cell 13, 2383–2396.

Gupta P, Gauthier NC, Cheng-Han Y, Zuanning Y, Pontes B, Ohmstede M, Martin R, Knolker HJ, Dobereiner HG, Krendel M, Sheetz M (2013). Myosin 1E localizes to actin polymerization sites in lamellipodia, affecting actin dynamics and adhesion formation. Biol Open 2, 1288–1299.

Hannigan M, Zhan L, Ai Y, Huang CK (2001). Leukocyte-specific gene 1 protein (LSP1) is involved in chemokine KC-activated cytoskeletal reorganization in murine neutrophils in vitro. J Leukoc Biol 69, 497–504.

Harrison RE, Sikorski BA, Jongstra J (2004). Leukocyte-specific protein 1 targets the ERK/MAP kinase scaffold protein KSR and MEK1 and ERK2 to the actin cytoskeleton. J Cell Sci 117, 2151–2157.

Howard TH, Hartwig J, Cunningham C (1998). Lymphocyte-specific protein 1 expression in eukaryotic cells reproduces the morphologic and motile abnormality of NAD 47/89 neutrophils. Blood 91, 4786–4795.

Howard T, Li Y, Torres M, Guerrero A, Coates T (1994). The 47-kD protein increased in neutrophil actin dysfunction with 47- and 89-kD protein abnormalities is lymphocyte-specific protein. Blood 83, 231–241.

Huang CK, Zhan L, Ai Y, Jongstra J (1997). LSP1 is the major substrate for mitogen-activated protein kinase-activated protein kinase 2 in human neutrophils. J Biol Chem 272, 17–19.

Jongstra J, Ittel ME, Iscove NN, Brady G (1994). The LSP1 gene is expressed in cultured normal and transformed mouse macrophages. Mol Immunol 31, 1125–1131.

Jongstra J, Tidmarsh GF, Jongstra-Bilen J, Davis MM (1988). A new lymphocyte-specific gene which encodes a putative Ca2+-binding protein is not expressed in transformed T lymphocyte lines. J Immunol 141, 3999–4004.

Jongstra-Bilen J, Janmey PA, Hartwig JH, Galea S, Jongstra J (1992). The lymphocyte-specific protein LSP1 binds to F-actin and to the cytoskeleton through its COOH-terminal basic domain. J Cell Biol 118, 1443–1453.

Jongstra-Bilen J, Misener VL, Wang C, Ginzberg H, Auerbach A, Joyner AL, Downey GP, Jongstra J (2000). LSP1 modulates leukocyte populations in resting and inflamed peritoneum. Blood 96, 1827–1835.

Jongstra-Bilen J, Young AJ, Chong R, Jongstra J (1990). Human and mouse LSP1 genes code for highly conserved phosphoproteins. J Immunol 144, 1104–1110.

Kadiyala RK, McIntyre BW, Krensky AM (1990). Molecular cloning and characterization of WP34, a phosphorylated human lymphocyte differentiation and activation antigen. Eur J Immunol 20, 2417–2423.

Klein DP, Galea S, Jongstra J (1990). The lymphocyte-specific protein LSP1 is associated with the cytoskeleton and co-caps with membrane IgM. J Immunol 145, 2967–2973.

Klein DP, Jongstra-Bilen J, Ogryzlo K, Chong R, Jongstra J (1989). Lymphocyte-specific Ca2+-binding protein LSP1 is associated with the cytoplasmic face of the plasma membrane. Mol Cell Biol 9, 3043–3048.

Krendel M, Osterweil EK, Mooseker MS (2007). Myosin 1E interacts with synaptojanin-1 and dynamin and is involved in endocytosis. FEBS Lett 581, 644–650.

Larsen EC, DiGennaro JA, Saito N, Mehta S, Loegering DJ, Mazurkiewicz JE, Lennartz MR (2000). Differential requirement for classic and novel PKC isoforms in respiratory burst and phagocytosis in RAW 264.7 cells. J Immunol 165, 2809–2817.

Larsen EC, Ueyama T, Brannock PM, Shirai Y, Saito N, Larsson C, Loegering D, Weber PB, Lennartz MR (2002). A role for PKC-epsilon in Fc gammaR-mediated phagocytosis by RAW 264.7 cells. J Cell Biol 159, 939–944.

Li SS (2005). Specificity and versatility of SH3 and other proline-recognition domains: structural basis and implications for cellular signal transduction. Biochem J 390, 641–653.

Li Y, Guerrero A, Howard TH (1995). The actin-binding protein, lymphocyte-specific protein 1, is expressed in human leukocytes and human myeloid and lymphoid cell lines. J Immunol 155, 3563–3569.

Li Y, Zhang Q, Aaron R, Hilliard L, Howard TH (2000). LSP1 modulates the locomotion of monocyte-differentiated U937 cells. Blood 96, 1100–1105.

Liu L, Cara DC, Kaur J, Raharjo E, Mullaly SC, Jongstra-Bilen J, Jongstra J, Kubes P (2005). LSP1 is an endothelial gatekeeper of leukocyte transendothelial migration. J Exp Med 201, 409–418.

Mansfield PJ, Shayman JA, Boxer LA (2000). Regulation of polymorphonuclear leukocyte phagocytosis by myosin light chain kinase after activation of mitogen-activated protein kinase. Blood 95, 2407–2412.

Matsumoto N, Kita K, Kojima S, Yamamoto K, Irimura T, Miyagi M, Tsunasawa S, Toyoshima S (1995). Lymphocyte isoforms of mouse p50 LSP1, which are phosphorylated in mitogen-activated T cells, are formed through alternative splicing and phosphorylation. J Biochem 118, 237–243.

Matsumoto N, Kojima S, Osawa T, Toyoshima S (1995). Protein kinase C phosphorylates p50 LSP1 and induces translocation of p50 LSP1 in T lymphocytes. J Biochem 117, 222–229.

Matsumoto N, Toyoshima S, Osawa T (1993). Characterization of the 50 kDa protein phosphorylated in concanavalin A-stimulated mouse T cells. J Biochem 113, 630–636.

Misener VL, Hui C, Malapitan IA, Ittel ME, Joyner AL, Jongstra J (1994). Expression of mouse LSP1/S37 isoforms. S37 is expressed in embryonic mesenchymal cells. J Cell Sci 107, 3591–3600.

Miyoshi EK, Stewart PL, Kincade PW, Lee MB, Thompson AA, Wall R (2001). Aberrant expression and localization of the cytoskeleton-binding pp52 (LSP1) protein in hairy cell leukemia. Leuk Res 25, 57–67.

Ouderkirk JL, Krendel M (2014). Myosin 1e is a component of the invadosome core that contributes to regulation of invadosome dynamics. Exp Cell Res 322, 265–276.

Palker TJ, Fong AM, Scearce RM, Patel DD, Haynes BF (1998). Developmental regulation of lymphocyte-specific protein 1 (LSP1) expression in thymus during human T-cell maturation. Hybridoma 17, 497–507.

Pust S, Morrison H, Wehland J, Sechi AS, Herrlich P (2005). Listeria monocytogenes exploits ERM protein functions to efficiently spread from cell to cell. EMBO J 24, 1287–1300.

Saksela K, Permi P (2012). SH3 domain ligand binding: what's the consensus and where's the specificity? FEBS Lett 586, 2609–2614.

Sechi A (2004). Molecular basis of Fcγ receptor-mediated phagocytosis: signalling to cytoskeleton remodelling and its subversion by pathogenic microorganisms. Recent Res Dev Cell Sci 1, 11–27.

Stöffler HE, Ruppert C, Reinhard J, Bähler M (1995). A novel mammalian myosin I from rat with an SH3 domain localizes to Con A-inducible, F-actin-rich structures at cell-cell contacts. J Cell Biol 129, 819–830.

Tanaka M, Gupta R, Mayer BJ (1995). Differential inhibition of signaling pathways by dominant-negative SH2/SH3 adapter proteins. Mol Cell Biol 15, 6829–6837.

Wang C, Hayashi H, Harrison R, Chiu B, Chan JR, Ostergaard HL, Inman RD, Jongstra J, Cybulsky MI, Jongstra-Bilen J (2002). Modulation of Mac-1 (CD11b/CD18)-mediated adhesion by the leukocyte-specific protein 1 is key to its role in neutrophil polarization and chemotaxis. J Immunol 169, 415–423.

Wong MJ, Malapitan IA, Sikorski BA, Jongstra J (2003). A cell-free binding assay maps the LSP1 cytoskeletal binding site to the COOH-terminal 30 amino acids. Biochim Biophys Acta 1642, 17–24.

Woolner S, Bement WM (2009). Unconventional myosins acting unconventionally. Trends Cell Biol 19, 245–252.

Wu Y, Zhan L, Ai Y, Hannigan M, Gaestel M, Huang CK, Madri JA (2007). MAPKAPK2-mediated LSP1 phosphorylation and FMLP-induced neutrophil polarization. Biochem Biophys Res Commun 358, 170–175.

Würflinger T, Gamper I, Aach T, Sechi AS (2011). Automated segmentation and tracking for large-scale analysis of focal adhesion dynamics. J Microsc 241, 37–53.

Zhang Q, Li Y, Howard TH (2000). Human lymphocyte-specific protein 1, the protein overexpressed in neutrophil actin dysfunction with 47-kDa and 89-kDa protein abnormalities (NAD 47/89), has multiple F-actin binding domains. J Immunol 165, 2052–2058.

Zhang Q, Li Y, Howard TH (2001). Hair-forming activity of human lymphocyte specific protein 1 requires cooperation between its caldesmon-like domains and the villin headpiece-like domains. Cell Motil Cytoskeleton 49, 179–188.